

OPTIMAL FRONTAL VEHICLE CRASH PULSES -- A NUMERICAL METHOD FOR DESIGN

Yibing Shi

Jianping Wu

Guy S. Nusholtz

DaimlerChrysler Corporation

USA

Paper Number 514

ABSTRACT

In a frontal vehicle crash, for a given crash velocity and given maximum vehicle crush, with a known restraint characteristic, what is the vehicle pulse, subject to lower and upper bound constraints, that produces the lowest peak occupant deceleration? A solution procedure using numerical optimization is proposed. The pulse is discretized in the vehicle crush domain. The optimization search is facilitated by a specially developed algorithm that is a hybrid of the sequential quadratic programming (SQP) algorithm for nonlinear constrained optimization and the genetic algorithm (GA). Optimization examples are shown with linear and nonlinear occupant restraints. Numerical results from the examples indicate that when the number of pulse discretization segments is less than five, the solution method is effective in providing pulse improvements for practical problems. A discussion on the theoretical and practical aspects of optimal pulses is also given, with reference to a theoretical optimal pulse recently published by Wu et al. [1].

INTRODUCTION

Occupant protection in vehicle crash is an important aspect in automobile design. It has been a continuing endeavor on the part of automobile manufactures. Some occupant crash-test responses are also regulated by crash safety standards in many countries and geo-political regions. Engineering design in this field is generally executed with integrated testing and analytical modeling. Analytical modeling at present generally includes finite element, rigid-body dynamics, and simple spring-mass model analyses. Each of these approaches reduces the vehicle-occupant restraint problem to a different level of abstraction that is best suited to answering questions raised from a particular perspective concerning the central occupant response issue. These predictive models, in their most direct applications, simulate the occupant response under given vehicle structure and restraint specifications. Given this capability, a question that is naturally expected is then: what is the best structure and restraint design for the occupant? This optimal design question is the focus of this study.

A definition of "best for the occupant" is in order at this point. What metrics most comprehensively and accurately reflect the level of occupant protection is in itself a topic that still requires considerable investigation. Nevertheless, the peak occupant thorax acceleration has been used in the industry. This metric has also been one of the injury assessment values in the US Federal Motor Vehicle Safety Standard 208 for frontal crash occupant protection. It serves as an indicator of the force acting on the occupant if the occupant is approximated as a single point mass. In the scope of this study, "best for the occupant" means a condition that gives the lowest possible peak occupant thoracic acceleration.

The frontal vehicle crash design optimization problem may be dealt with analytically with two approaches. The first would use *physical vehicle parameters* as the optimization variables, and would therefore involve the solution of the dynamic crash response of the vehicle in addition to the solution of the occupant response to the vehicle motion. This makes an efficient and accurate structural dynamic solver a prerequisite, which at the present time, still represents a challenge. The alternative approach is to use a two-step strategy by first finding an optimal *structural response* for the occupant. The second step is to either solve an inverse structural design problem based on the optimal structural response, or provide a direction for structural design. The study in this paper assumes this two-step approach, and deals only with the first step, i.e., finding the *optimal structural crash response* for the occupant.

Many studies have been published in the last three decades or so on this optimal pulse problem. Several [1-11] of these are particularly relevant to the current work, and a brief review is given here. In [2-3], different simple theoretical vehicle acceleration pulses are evaluated analytically in terms of their effect on the occupant. In contrast, in [4-9], numerical methods are used to compute the occupant response (based on either single-degree-of-freedom (SDOF) spring-mass model or multi-body occupant dynamics simulation), allowing for vehicle pulses of general shapes. The vehicle pulses are in general pre-selected for evaluation; therefore, these are not optimization studies in the sense of the lack of an automatic search. In [10], a sensitivity analysis is used, which is in essence a gradient-based iterative search. The vehicle pulse is discretized in the crash displacement domain. Overall, to date, the optimal

pulse problem has not been addressed using a formal optimization approach as far as the authors are aware.

Results of several studies [6,10] have shown that a "good" pulse has the following characteristics: high at the beginning stage, decreasing to very low levels, and re-surfing in the last stage of the crash. However, the authors did not present a definitive explanation from a fundamental basis.

Motozawa and Kamei [11] used a specific condition to identify "optimal pulses" with a linear SDOF spring-mass model. Essentially the condition stipulates the vehicle pulse to have a transient period in the beginning that brings the occupant acceleration to a level, *and* be able to maintain this level to the end of the crash. A family of pulses satisfying this condition were identified, which were concluded to "consist of three aspects: high deceleration, low or negative deceleration, and constant deceleration".

Wu et al. [1] recently presented SDOF spring-mass model analyses that addressed the optimal pulse problem by applying an energy relationship between the vehicle pulse and the occupant acceleration in the occupant-vehicle relative motion domain. A significant result in [1] is the answer to the optimal pulse question: for a given amount of vehicle crush under a given crash velocity, the optimal pulse is one that consists of an impulse, a subsequent zero-acceleration period, and finally a constant level period. This is applicable to both linear and nonlinear non-decreasing restraint functions. The velocity change of the impulse, the timing of the zero acceleration period, and the final constant level are completely determined by the crash velocity, the maximum crush, and the restraint function. This result is significant because it shows that the results of several existing studies [9-11] can all be unified as specific cases along the path to this optimum (i.e., it is the theoretical limit of all those results). Physically, the optimality of this "high-ended" pulse derives from its unique ability to bring the restraint as quickly as possible to a peak level, and maintain it at this level for the rest of the crash event (i.e., a near square-shaped occupant acceleration response in the time domain, which is the most efficient).

At this point, the aspect of constraint condition deserves some discussion. Figure 1 shows the normalized linear occupant restraint system energy (which maps directly to the peak occupant acceleration) as dependent on the normalized maximum vehicle crush for several types of pulses. Clearly, the notion of optimal pulse is only meaningful when we specify all the constraints, for

example, under a given amount of total vehicle crush. Further constraint conditions are necessary to narrow down the optimal pulse to one relevant to a particular case. For example, the fourth pulse shown in Figure 1, which is a case in the family of pulses given in [11], is inadmissible if the vehicle pulse is constrained to be non-negative (Note that the thin part of the dashed line corresponds to pulses with the vehicle velocity and/or the crush having a negative period before the end of the pulse. These are not realistic in a physical vehicle crash case). As a further example showing the importance of constraints, the lower "Two-Impulse" curve (ending time (t_e) longer than a quarter of the period) in Figure 1 will become the higher one, if a constraint is imposed that the occupant does not experience unloading (see Appendix 1).

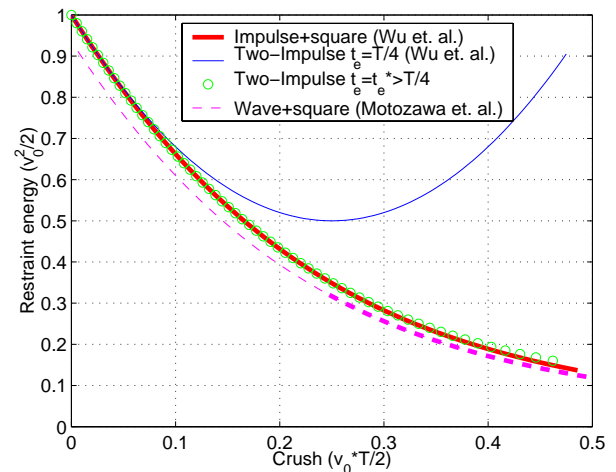


Figure 1. Occupant restraint energy and crush pulse relationship for selected pulse examples for linear restraint (Occupant restraint energy is normalized by that corresponding to a single impulse pulse; and vehicle crush is normalized by that corresponding to a square pulse ending at the natural period of the restraint system (T). v_0 denotes the crash velocity).

In summary, the optimal pulse question can not stand alone; it is only meaningful when the appropriate constraints are specified. The answer, under the equal maximum crush and non-negative constraints, is given in [1] as the theoretical optimal pulse for a general restraint system. In practice, the optimal pulse question becomes somewhat more complicated. Inevitably there will be more constraints; for example, there may be limits to the acceleration that will exclude the possibility of an impulse at the beginning of the theoretical optimal pulse. An

approach to obtain a solution which can deal with such practical constraints is the objective of this study. A numerical optimization method is proposed, and applications of this method to practical examples are shown.

NUMERICAL OPTIMIZATION METHOD

Problem Definition

The preceding discussion suggests that the optimal pulse question can be cast as a constrained nonlinear optimization problem. The peak value of the entire acceleration time history of the occupant is chosen here as the objective function (although the general numerical solution method used here does allow other metrics based on the kinematics of the occupant, for example, its peak relative velocity, or the maximum work to it from the restraint). The vehicle pulse will be the variable to be optimized, subject to the appropriate constraints (for example, in the form of maximum crush, etc.).

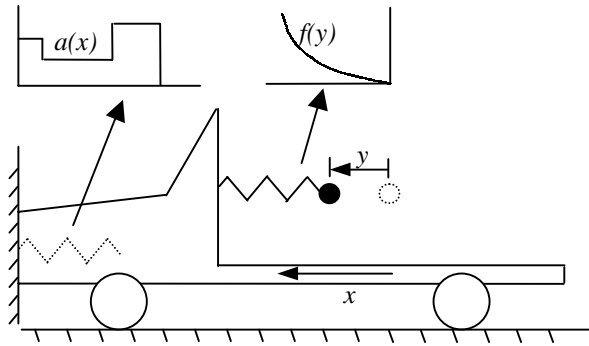


Figure 2. Schematic picture describing the system and sign convention (x represents vehicle crush, and y represents relative motion between the occupant and the vehicle, with positive direction shown by the arrows. Vehicle acceleration versus crush, and occupant acceleration versus relative motion relationship are shown schematically).

The above description can be summarized as:

$$\begin{aligned} & \underset{x}{\text{minimize}} \underset{t}{\text{maximum}} (\ddot{x}(t) + \ddot{y}(x(t))), \\ & \text{subject to constraint } g(x) = 0 \end{aligned} \quad (1),$$

where x is the forward motion of the vehicle (crush), y is the forward motion of the occupant relative to the vehicle (see Figure 2), and g denotes constraints that can be put on the acceleration of the vehicle.

Since the optimization variable is the vehicle pulse $x(t)$, a function by itself, the above-defined optimization problem is, strictly speaking, a *functional* optimization problem. Since it is difficult, if not impossible, to explicitly express the peak occupant acceleration (the functional) in terms of the vehicle pulse, with the constraint, and with a general restraint function, the preferred analytical approach of finding and solving the Euler equation that corresponds to the optimal condition is impractical. Therefore, in this study, the vehicle pulse is discretized, and represented by individual acceleration levels as variables. This approximation turns the *functional* optimization problem into a simpler *parameter* optimization one.

The discretization of the pulse is carried out in the vehicle acceleration-crush domain, instead of the time domain. This is for two reasons. First, a specification in this domain, as opposed to in the time domain, is natural to structural design since the acceleration versus crush information is directly mapped to force levels of each segment of the structure along its longitudinal axis. Second, the imposition of the constraints is more convenient in this domain, as will be seen later.

The relationship between y (relative motion) and x (vehicle crush) is implicitly defined by the following two simple second order ordinary differential equations (ODE):

$$\begin{aligned} \ddot{y} + f(y) &= -\ddot{x}, \\ \ddot{x} &= -a(x) = -a(x; [x_i; a_i]) \quad (i=1, \dots, n) \end{aligned} \quad (2).$$

The first equation is the equation of motion for the occupant, where $f(y)$ is the restraint force normalized by the mass of the occupant ($f(y) > 0$, when $y > 0$). (For simplicity, the restraint force is assumed to depend only on the relative position of the occupant throughout this study, although numerically, damping and other rate-dependent behavior can also be incorporated).

The second equation relates the time domain function $x(t)$ to the crush domain defined vehicle acceleration $a(x)$ ($a(x) > 0$ when $x > 0$, for frontal crash), and the second part of the equation denotes the discretization of the pulse into n segments, as shown in Figure 3. The crush distances x_i ($i=1, \dots, n$) that define the discretization are prescribed, and the n acceleration levels a_i are left as the parameters to be optimized. In all the computation in this paper, a rebound acceleration is assumed that has the same level as the

last segment of the crush pulse, and produces a rebound velocity of 1/10 of the crash velocity.

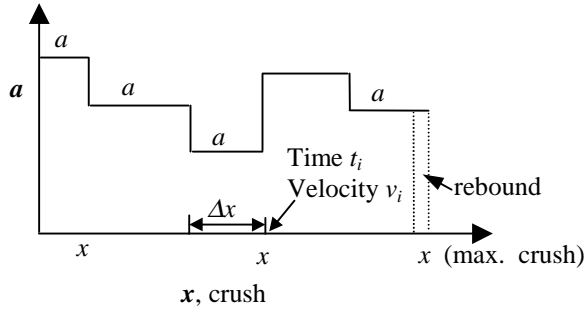


Figure 3. Discretization of the pulse in vehicle crush domain.

The initial conditions for the two equations are:

$$\begin{aligned} y(0) &= 0, & \dot{y}(0) &= 0, \\ x(0) &= 0, & \dot{x}(0) &= v_0 \end{aligned} \quad (3),$$

where v_0 is the initial crash velocity of the vehicle.

Throughout this study, the optimization constraints are the crash velocity (v_0) and the maximum crush (d_0). The velocity constraint can be written in terms of the optimization parameters a_i through the energy relationship as:

$$\sum_{i=1}^n \Delta x_i a_i - v_0^2 / 2 = 0 \quad (4).$$

The maximum crush constraint is automatically satisfied by discretizing the crush over the range $[0, d_0]$, which is the aforementioned second reason for formulating the problem in the acceleration-crush domain.

As discussed in the introduction, constraint on the pulse levels is also necessary for the problem to be physically meaningful. The constraint imposed in this study is:

$$a_{il} \leq a_i \leq a_{iu} \quad (i=1, \dots, n) \quad (5),$$

where a_{il} and a_{iu} are the lower and upper bounds for the i -th segment of the crash pulse. They are inputs to the computation and can be determined based on physical considerations (e.g., non-negative acceleration), or design limitations.

So far, the optimization problem has been fully defined. As a summary: a peak occupant acceleration can be obtained after solving Equations (2), under a given restraint function $f(y)$, with the initial conditions (3), for a given set of a_i that is defined

over a prescribed division of the total crush d_0 and subject to the constraints (4) and (5). The remaining task now is to develop an algorithm that facilitates the search for the optimal set of a_i .

Optimization Search Algorithm

The sequential quadratic programming (SQP) [12] has been established as an effective general nonlinear, constrained optimization algorithm. A brief account of the key strategies for the SQP is given here. The constrained optimization problem is transformed into an unconstrained using the Lagrangian function. The SQP algorithm goes through a sequence of iterations, progressively seeking to move to a better solution point. At each iteration, the problem is approximated by a quadratic programming (QP) sub-problem which can be precisely solved if the first and second order derivatives of the objective function are known. Commonly, the gradient (first order derivative) is approximated by finite difference, and the Hessian matrix (second order derivative matrix) and its update are also approximated for computational efficiency. With most implementations, the QP sub-problem provides only a search direction, and a step size along this direction is determined by evaluating a merit function that combines the objective function value and the amount of constraint violation. In the current study, a routine (*constr*) in the Matlab Optimization Toolbox [13] is adopted with modifications to the merit function definition and convergence criteria.

Computation of examples during the course of this study showed that the SQP algorithm by itself often converges (a sufficiently small step *and* objective function change in successive iterations) to local minima. While no method is known that completely eradicates this shortcoming, some strategies, often heuristic, do help alleviate the predicament. In this study, a "confirmation" step is implemented at the convergence of a SQP sequence, by invoking a simple genetic search algorithm (GA, see [12] for an introduction). The GA search explores a neighborhood of the SQP-converged point in the parameter space. If within a given amount of exploratory stochastic sampling, no superior point is identified, the SQP-converged point is confirmed, and the entire search is terminated; On the other hand, if the GA converges to a superior point, the control algorithm then recursively initiates the SQP/GA process using this point as the new starting point. The recursion goes on until a subsequent GA confirms a SQP convergence.

The GA-type of search schemes are function-value-comparison-based, with no derivative computation. It

attempts to move to improved points through a series of generations, each being composed of a population which has a set number (population size, 30 in this work) of individuals. Each individual is a point in the parameter space (in our case, a pulse). The schemes that are applied to the evolution of the generations have some analogy to the natural genetic evolution of species, hence the term *genetic*. Most evolution schemes consist of basic operations commonly named "reproduction", "cross-over", and "mutation". The reproduction ensures that fitter individuals (those giving better objective function values) get a higher probability of continuation into the new generation. The crossover operation provides some controlled randomness in the new population by combing "genes" (bits in the numerical representation of a parameter. The parameters are represented in the binary form in this study) from different individuals. The mutation operation, when applied, injects an additional measure of dynamics to the new population by completely reversing certain gene segments of a certain percentage of the individuals.

The GA is generally applied to unconstrained problems, since constraints, aside from the upper and lower bounds of the optimization variables, are difficult to implement in the GA. This is because some of the operations, such as the crossover and mutation, do not automatically preserve constraints. In this study, in order to use the GA, an *ad hoc* extra operation was devised so that the constraint equation (4) is enforced. This is possible, due largely to the simplicity of the constraint. This extra operation consists of a scaling and a bounding step. The scaling step simply scales an individual after the three GA operations mentioned above by a factor that brings the energy of the new individual to the crash energy (the second term of Equation (4)). Such a scaling preserves the "look" of each individual, which is a desirable property. The bounding step ensues that each individual is bounded. This is achieved by iteratively "trimming" the out-of-bound parameters and "re-distributing" the trimmed energy uniformly to the rest which are not at their respective bounds, until all the parameters are bounded.

Numerical Assessment of SQP/GA Algorithm

An example problem was solved using the above-proposed algorithm to assess its numerical effectiveness. The parameters that specify the problem were chosen to be representative of a possible car on the road today in a $v_0=15.56$ m/s (35 mph) full rigid barrier frontal crash. The maximum vehicle crush was $d_0=0.71$ m (28 inches). The restraint system was assumed to be linear, with

$\omega^2=1800$ (rad/s)² (ω being the fundamental radian frequency of the system). In order to assess convergence with different degrees of discretization, optimization runs were carried out for each of the following numbers of segments (c.f. Figure 3 for definition of n), $n=2, 3, 4, 5, 6, 8, 10, 15, 20$. For this example, the segment size was assumed to be equal, although the program allows for non-uniform division (as shown with a later example). For simplicity, the initial starting pulse in the acceleration-crush space, which was needed in the optimization, was uniform over all the segments (i.e., a square-pulse), whose magnitude was determined by:

$$a_{0i} = a_0 = \frac{1}{2} \frac{v_0^2}{d_0}, \quad (i=1, \dots, n) \quad (6).$$

A lower bound of 0, and upper bound of na_0 were specified for all the acceleration segments (Trial numerical runs with negative lower bounds produced better acceleration results, consistent with the discussion in the Introduction).

Preliminary runs showed that repeat runs for the same problem (same n) did not converge to the same point, because of the randomness of the GA part of the hybrid algorithm. As a result, for each problem (a given n), ten repeat SQP/GA runs were executed to get a "statistical" assessment. In addition, one SQP-only run was executed for comparison.

Because of the number of runs involved, there was a motivation to increase the speed of the execution. As a result, in the algorithm development stage, the integration of the equations of motion (Equation (2)) was carried out analytically as detailed in Appendix 2. This is possible because a linear-elastic restraint was assumed. In the following, results from this "analytical" approach are presented, and correspondingly noted. After the algorithm development stage, the equations of motion (Equation (2)) were solved using a numerical ODE solver in Matlab (*ode45*). This ODE-solver approach was applied to this example problem, and all the rest of the numerical examples shown in this paper. It is noted that in using this approach, the restraint was assumed to be linear in loading, but the unloading was chosen to be a straight line from the unloading point with a slope 5 times that of the loading part. This more realistic restraint model was afforded by the flexibility of the numerical ODE-solver method.

Figure 4 shows the result of the numerical study described in the last few paragraphs. At each of the n values where computation was carried out, result of

the optimal peak occupant acceleration from the one SQP-only run is shown by the "star" plot symbol. The problem of convergence to local minimum is reflected in the figure (e.g., $n=10$ result is inferior to $n=5$ result). At each n value, the ten hybrid SQP/GA runs in general provided improvements over the SQP-only run; however, the ten runs did not end at the same point (note that each of the result is still a converged point, therefore, a minimum). The dashed line in Figure 4 passes through the average of the ten hybrid runs at each n value, giving an estimate of the expected value from the hybrid algorithm. It is noted that at relatively small n values (e.g., $n=2, 3, 4, 5$), the SQP was able to produce relatively good solutions, but as n gets larger, help from the GA step becomes necessary to take the solution out of a local minimum and continue the iteration.

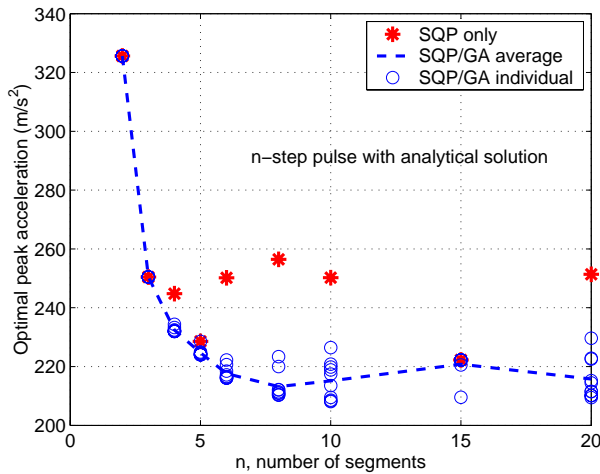


Figure 4. Convergence study with different number of discretization segments (At each n value, ten SQP/GA run results are shown by circle symbols. Some of the ten symbols overlap and can not be distinguished, as in the cases of $n=2$, and $n=15$, etc.).

Numerical convergence is further examined with Figure 5a which shows the case of $n=5$ as an example. Each of the ten hybrid runs started with the same path as the SQP-only run in the very first SQP step, but embarked on different paths during the subsequent GA, and the next SQP/GA iterations. Figure 5b presents the vehicle accelerations corresponding to the runs shown in Figure 5a in the vehicle crush domain (normalized by the maximum crush, d_0).

Parallel to Figures 5a and 5b, Figures 6a and 6b show the same type of information for the case of $n=10$, as an example. Note that in Figures 5a and 6a, only the

history of the SQP phase of the SQP/GA iteration is shown with respect to the cumulative number of the SQP internal iteration, while the history of the GA phase is not shown and essentially collapses in this plotting scheme. As a result, a sudden drop (c.f. Figure 6a) signifies an appreciable improvement from a GA phase. The number of SQP/GA iterations and the total number of function evaluations as a measure of the amount of computation for this series of runs are provided in Table 1.

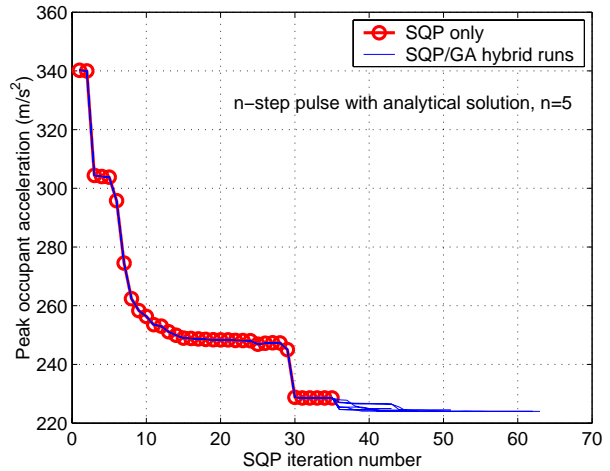


Figure 5a. Convergence history of runs with $n=5$ (One line is plotted for each of the ten SQP/GA hybrid runs, although they are difficult to distinguish).

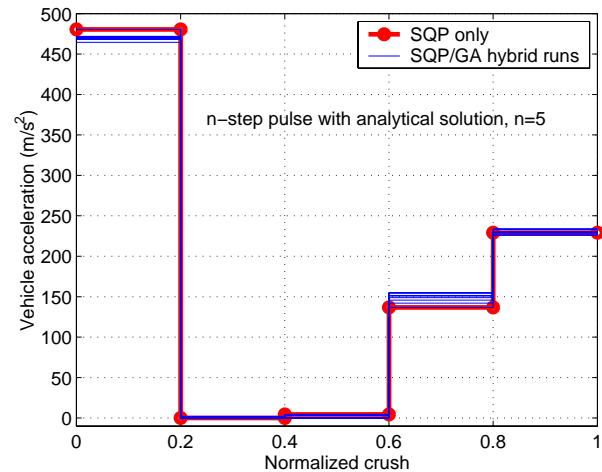


Figure 5b. Vehicle acceleration corresponding to runs shown in Figure 5a (One line is plotted for each of the ten SQP/GA hybrid runs, although they are difficult to distinguish. Vehicle crush is normalized by the maximum crush, d_0 , for plotting. The dot plot symbols on the SQP run result signify the discretization of all the runs shown).

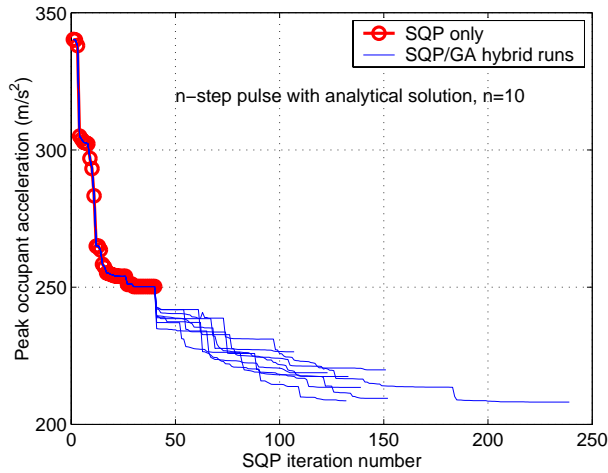


Figure 6a. Convergence history of runs with $n=10$ (The sudden drops at 40 iterations for the hybrid runs correspond to the improvement from the first GA).

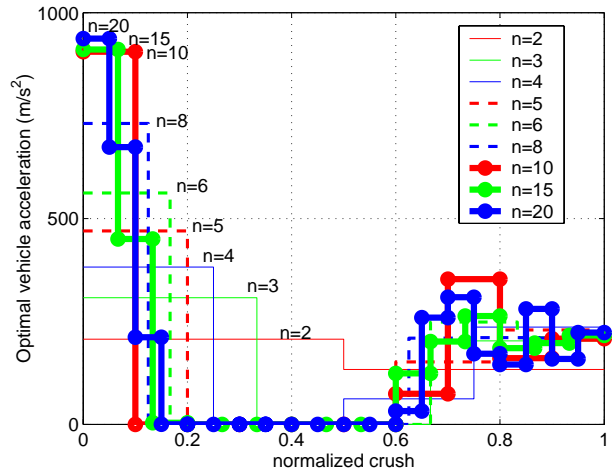


Figure 7a. Vehicle acceleration result of the best of the runs under each n value shown in Figure 4. (The dot plot symbols signify the discretization).

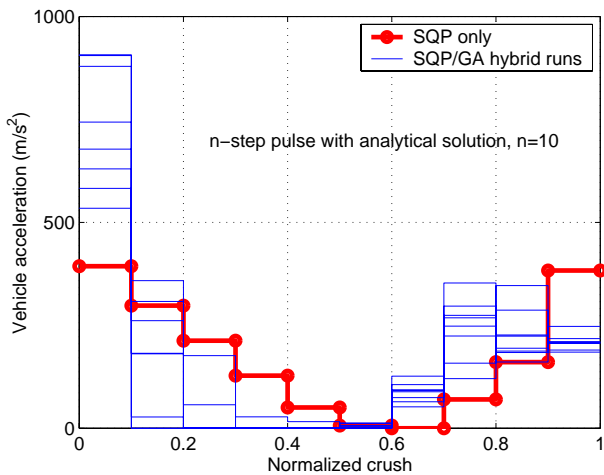


Figure 6b. Vehicle acceleration corresponding to runs shown in Figure 6a (The dot plot symbols of the SQP-only run signify the discretization of all the runs shown).

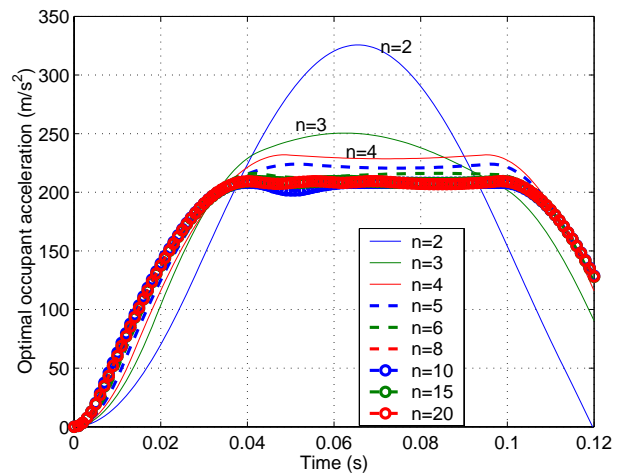


Figure 7b. Occupant acceleration time history corresponding to pulses shown in Figure 7a (The dot plot symbols correspond to the 1 ms time-step size in the analytical solution in the optimization).

As a summary, Figure 7a shows the optimal pulse result from the runs shown in Figure 4, and Figure 7b presents the corresponding occupant acceleration time history. Although the curves are difficult to distinguish in Figure 7a, the objective is to show that as the pulse is allowed more flexibility (i.e., n increases), the optimal pulse progressively has a higher and narrower peak at the beginning of the crush, which is followed by a near-zero acceleration part, and a more moderate elevation in the end. Figure 7b shows that the optimal occupant response gradually approaches a "hat" shape as n increases.

After the algorithm development with the above "analytical" approach, the same problem was solved using the ODE-solver approach, which is necessary for general non-linear occupant restraints. The main results are shown in Figure 8, and iteration details given in Table 2 (The computation time per function evaluation increased by two orders of magnitude on average). The convergence trend is similar (Figure 8a v.s. Figure 4), but a degradation is seen relative to the "analytical" runs, when n is relatively large. This appears to be caused by minor inaccuracy in the gradient calculation, which itself is caused by otherwise inconsequential numerical inaccuracy in

Table 1.
Number of function evaluations for convergence study runs with "analytical" equation of motion solution

	n=2			3			4			5			6			8			10			15			20		
	ns	nr	ng	ns	nr	ng	ns	nr	ng	ns	nr	ng	ns	nr	ng	ns	nr	ng	ns	nr	ng	ns	nr	ng	ns	nr	ng
Run 0	152	0	-	87	0	-	132	-	-	231	-	-	248	-	-	399	-	-	587	-	-	1500	-	-	1567	-	-
Run 1	152	0	1200	87	0	1200	644	2	3600	408	1	2400	1130	3	4800	2650	3	4800	3786	4	6060	1500	0	1200	7169	3	4920
2	152	0	1200	87	0	1200	313	1	2400	231	0	1200	639	1	2400	1968	4	6000	2321	3	4800	1500	0	1200	4186	3	4800
3	152	0	1200	87	0	1200	407	2	3600	474	1	2400	1295	2	3600	1707	2	3600	2185	3	4920	2230	1	2400	8173	4	6120
4	152	0	1200	87	0	1200	360	2	3600	417	1	2400	1301	4	6000	2178	4	6000	2533	4	6030	3000	1	2460	5580	2	3600
5	152	0	1200	87	0	1200	432	2	3600	378	1	2400	816	2	3720	1717	3	4800	2039	2	3780	1500	0	1200	9987	5	7200
6	152	0	1200	87	0	1200	498	1	2400	511	1	2400	1119	2	3690	1808	3	4800	2362	2	3660	1500	0	1200	5590	2	3600
7	152	0	1200	87	0	1200	452	2	3600	358	1	2400	633	2	3840	1921	2	3660	2343	3	4800	1500	0	1200	10383	7	9600
8	152	0	1200	87	0	1200	519	2	3600	472	1	2400	1526	3	4800	1466	2	3600	1484	1	2400	1500	0	1200	7839	4	6150
9	152	0	1200	87	0	1200	242	1	2400	487	1	2400	1167	2	3600	2662	4	6000	1992	2	3600	1500	0	1200	7584	3	4860
10	152	0	1200	87	0	1200	475	3	4800	383	1	2400	851	2	3600	1886	2	3600	2917	3	4800	1500	0	1200	4889	2	3600

Notes: n=2,3, ..., 20 indicates the number of segments for the series of runs.

ns: total number of function evaluations by the SQP phases of the hybrid algorithm; nr: number of SQP/GA recursions

ng: total number of function evaluations by the GA phases of the hybrid algorithm

Run 0 is SQP only and Run 1, 2, ..., 10 are repeat hybrid runs.

Table 2.
Number of function evaluations for convergence study runs with ODE equation solution

	n=2			3			4			5			6			8			10			15			20		
	ns	nr	ng	ns	nr	ng	ns	nr	ng	ns	nr	ng	ns	nr	ng	ns	nr	ng	ns	nr	ng	ns	nr	ng	ns	nr	ng
Run 0	200	0	0	300	0	0	242	0	0	500	0	0	600	0	0	547	0	0	1000	0	0	1338	0	0	2011	0	0
Run 1	200	0	1200	300	0	1200	368	1	2400	890	2	3600	2199	4	6000	3374	6	8400	1418	1	2400	5997	4	6000	7490	3	4980
2	200	0	1200	300	0	1200	368	1	2400	1173	2	3660	2317	5	7200	856	1	2400	3131	3	4800	5711	5	7200	12900	6	8400
3	200	0	1200	300	0	1200	819	3	4800	1356	2	3600	1900	4	6060	1941	4	6120	3312	3	4830	4289	3	4800	12035	5	7350
4	200	0	1200	300	0	1200	347	1	2400	1987	5	7200	1035	2	3600	2165	3	4800	3236	5	7230	5510	3	4860	10059	4	6000
5	200	0	1200	300	0	1200	368	1	2400	1173	2	3660	2317	5	7200	856	1	2400	3131	3	4800	5711	5	7200	10011	4	6000
6	200	0	1200	300	0	1200	642	1	2400	1004	1	2430	1379	3	4950	2575	4	6000	3789	5	7200	4723	4	6000	7195	3	4800
7	200	0	1200	300	0	1200	781	2	3600	1045	2	3600	1712	4	6150	1541	2	3600	3508	4	6060	3393	2	3660	7489	3	5100
8	200	0	1200	300	0	1200	787	2	3600	946	1	2400	1312	2	3630	2347	4	6000	3581	4	6030	5295	4	6000	23987	14	18000
9	200	0	1200	300	0	1200	335	1	2550	1176	2	3600	1378	3	4800	1625	2	3810	2028	2	3600	5101	4	6000	4881	2	3600
10	200	0	1200	300	0	1200	377	1	2400	1017	2	3600	1486	3	4920	1185	1	2400	1506	1	2400	3616	3	4890	18022	8	10800

function value evaluation by the ODE solver. The "best-case" results (Figures 8b and c) are less orderly compared with the "analytical" solutions. The ODE-solver approach was used in all the computation shown in the rest of this paper, with n limited to 5.

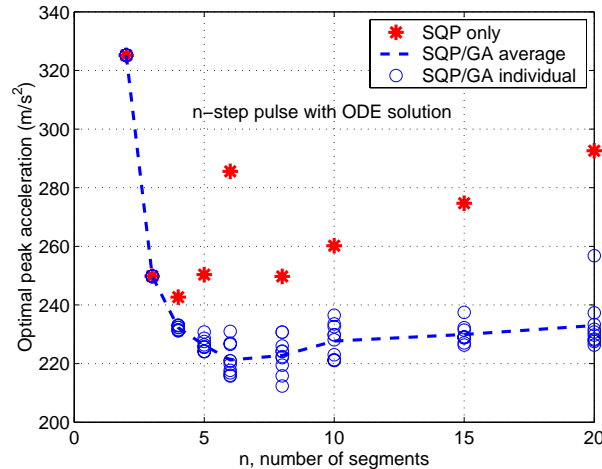


Figure 8a. Convergence study of different number of discretization segments, using ODE solver (At each n value, ten SQP/GA run results are shown by circle symbols. Some of the ten symbols overlap and can not be distinguished).

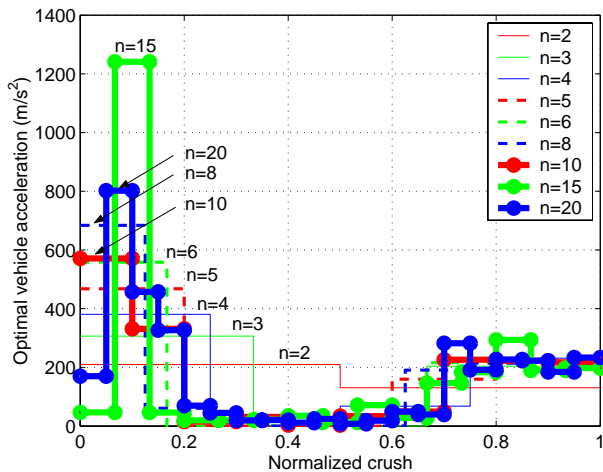


Figure 8b. Vehicle acceleration result of the best of the runs under each n value shown in Figure 8a (The dot plot symbols signify the discretization).

APPLICATION EXAMPLES

Two examples were run to demonstrate the application of the numerical optimization method. The first example involved a nonlinear occupant restraint function (This restraint function was used in [1]. In the present numerical study, a very small positive slope is given to the flat part of the restraint at 400 m/s^2 (40 g) to build in a gradient in the

objective function). It used the same problem definition parameters (initial velocity and maximum vehicle crush), and optimization parameter bounds as the preceding algorithm study example. Four discretization possibilities, $n=2, 3, 4,$ and 5 , each with

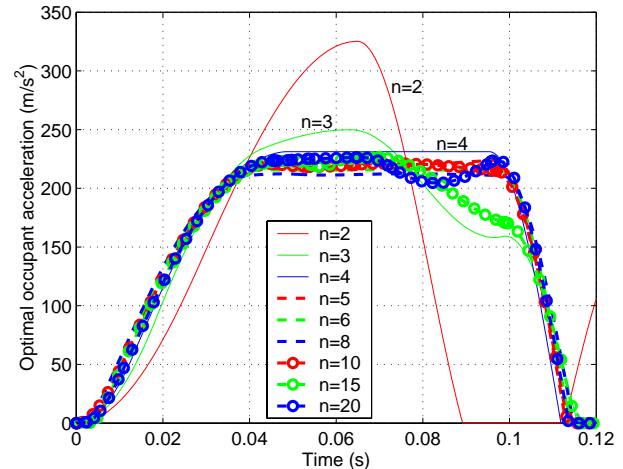


Figure 8c. Occupant acceleration time history corresponding to pulses shown in Figure 7a (The difference between curves shown here and those in Figure 7b in the unloading phase is a result of the difference in the restraint unloading assumption).

ten repeat SQP/GA runs, were executed to further examine the numerical behavior of the algorithm. Each optimization run still started with the convenient square pulse. The results are shown in Figure 9.

In Figure 9a, the ten repeat run results at each of the n values are shown, with the dashed line going through the averages. Up to $n=4$, the ten repeat runs resulted in identical peak occupant acceleration values (and identical pulses). Also note that for $n=4$, the ten SQP/GA runs did not follow exactly the same path during the iteration, but concluded at the same point). By $n=5$, the algorithm started to have difficulty converging to a single solution, with one of the runs standing out clearly. The actual pulses for the $n=4$ and $n=5$ cases are shown in Figure 9b. (The pulses corresponding to the lowest ("best") and the highest ("worst") occupant peak acceleration values are identified in Figure 9b). The resulting occupant acceleration in the time and relative displacement domains are shown in Figures 9c and 9d respectively, along with that by the initial square pulse. This example shows that the algorithm deals with general nonlinear restraint correctly, and good convergence appears to be attainable for at least up to $n=4$ segments for the pulse.

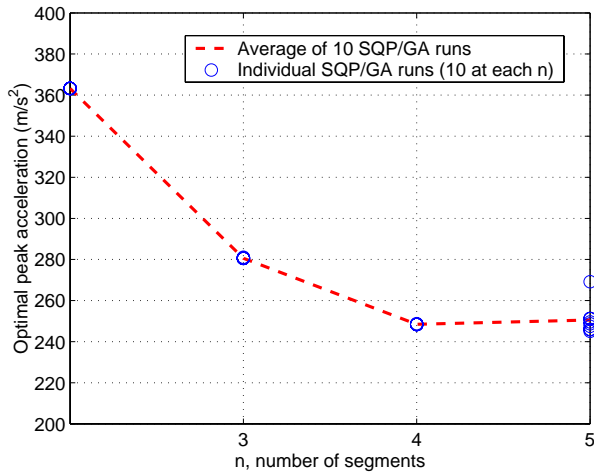


Figure 9a. Result of nonlinear restraint application example (There are ten circles (runs) at each of the n values).

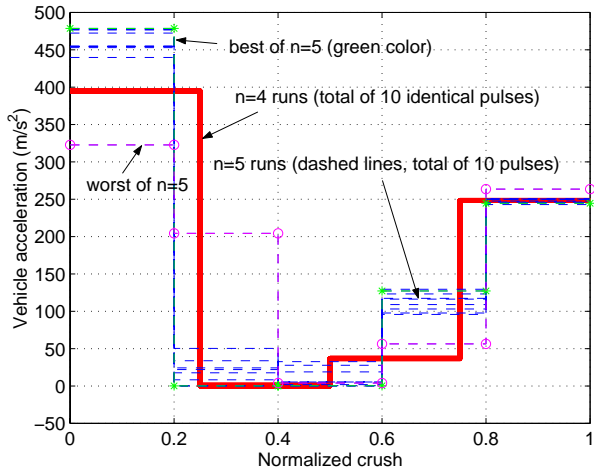


Figure 9b. Results of $n=4$ and $n=5$ runs of the nonlinear restraint application example

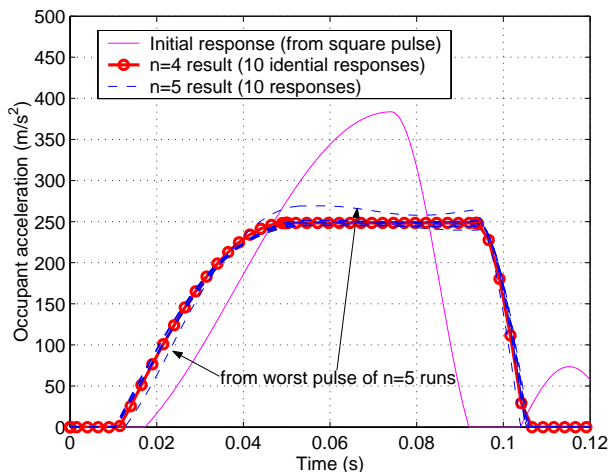


Figure 9c. Occupant acceleration time history of nonlinear restraint application example (The

spacing of the circle plot symbol is ten times the step size of the ODE solver in all the optimization runs.)

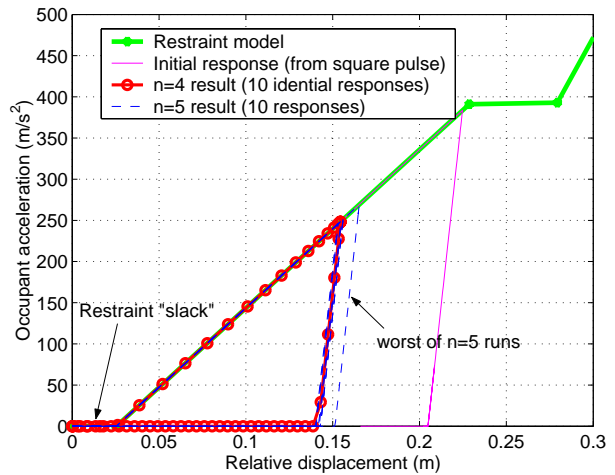


Figure 9d. Nonlinear restraint model (loading part) and occupant response in relative displacement domain (The restraint model includes a linear unloading part, the slope of which is shown by the numerical results in the figure. See Figure 9c for an explanation of the circle plot symbols.)

The second application example is a pulse shaping scenario: when a vehicle crash test has been carried out, what changes to the pulse could be made to minimize the occupant peak acceleration, if the total vehicle crush and the occupant restraint systems are fixed? This example used data from an actual 56 kph frontal rigid barrier crash test. A four-segment vehicle pulse model was constructed in the crush domain, and it was used as the starting point for the optimization. An occupant restraint system model was also extracted from test data. The optimization was carried out for the four acceleration levels, which were subject to lower and upper bounds that were assumed to reflect possible limitations. The result of the computation is shown in Figure 10 along with the actual test response and the input model. (In terms of computational details, ten repeat runs were executed. For this particular problem, each run converged with 23 major SQP iteration totaling 290 function evaluations. The GA part which consisted of 40 generations of population size 30 did not identify an improvement in any of the ten runs. Therefore, an identical result was obtained for all ten runs. Data shown in Figure 10 give this single result.)

The initial model of the pulse in the crush domain is shown in Figure 10a, and the restraint system model shown in Figure 10b. The pulse and restraint models produce an occupant response (which is the initial

starting point of the optimization) reasonably close to the actual test result in both history and the peak value, as shown in Figures 10b and 10c. The final optimized pulse is shown in Figure 10a, and the corresponding occupant responses shown in Figures 10b and 10c.

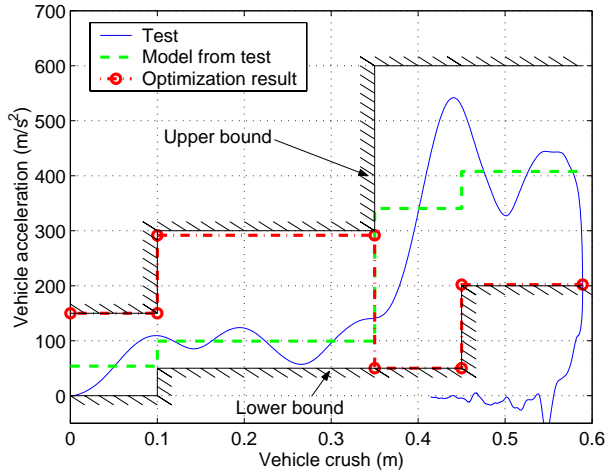


Figure 10a. Vehicle pulse and optimization bounds for application example.

The optimized pulse reached the upper bound in the first segment, and reached the lower bound in the third segment (note that numerically, the second segment of the pulse, at 291.65 m/s^2 , should not be considered reaching the upper bound set to 300 m/s^2 -- a quick numerical test that sets it to the upper limit and takes off the increased energy from the last segment produced occupant peak acceleration of 369.97 m/s^2 , higher than the 368.34 m/s^2 by the optimal pulse). From Figure 10c, the effect of the optimal pulse on the occupant response is to induce an earlier (in time) restraint. The amount of restraint energy reduction can be judged from Figure 10b.

DISCUSSION

Optimal Pulse Shape

Some of the optimization results here can be compared with the theoretical optimal. Figure 11, which follows the same format as Figure 1, shows the result of the series of runs with increasing n with the ODE solver shown in Figure 8a. The numerical results are normalized and represented by the circles in Figure 11. The result of this series of runs brings the occupant restraint energy from the square pulse at the chosen normalized vehicle crush down towards the theoretical optimal pulse by Wu et al. [1]. In theory, if global convergence is achieved consistently with increasing n , the result of this series of runs should eventually approach this line. This series of

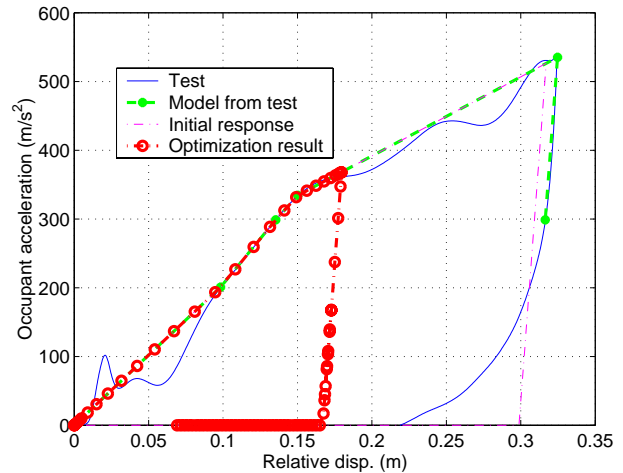


Figure 10b. Occupant restraint response for application example (The loading part of the restraint model consists of 4 linear pieces, and the unloading is specified as a straight line with slope shown by the last segment of the restraint model curve. For the optimization result, the circle plot symbols represent the computation data points, with a reduction factor of ten in frequency for clarity).

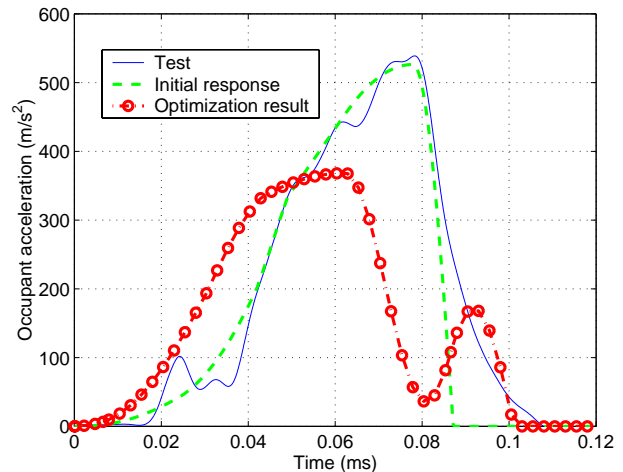


Figure 10c. Occupant acceleration time history (For the optimization result, the circle plot symbols represent the computation data points, with a reduction factor of ten in frequency for clarity.)

"optimal" pulses under a given n value achieve optimality by producing an occupant acceleration time history (see Figure 7b) that ramps to a plateau with a minimum vehicle crush permissible by the pulse shape requirement (e.g., n segments) and subject to non-negative pulse constraint. At the plateau, the occupant and the vehicle decelerate with the same acceleration while maintaining zero relative velocity.

In Figure 11, data are also presented on the optimal two-step pulse for a perspective. As with the other theoretical pulses shown in Figures 1 and 11, an analytical optimal solution could be derived, but with some added complexity. To avoid this, and to utilize the optimization method proposed here, the two-step optimal pulse was determined numerically. The n -step optimization routine (with the analytical equation solution for execution speed) was adopted with modifications. In this two-step pulse case, the division point of the two crush segments was also included as an optimization variable. To this end, a third optimization variable, the ratio of the first to second segments of crush displacement (in addition to the two acceleration steps) was added to the optimization variable list. Another modification involved normalizing the two acceleration step values by the square-pulse level, outside the search routine, to bring their magnitudes in parity with the third variable, which has lower and upper bounds of 0.0 and 1.0. To map out a curve, computation was carried out at each of ten normalized total vehicle crush values from 0.1 to 1.0. At each of these values, to gain confidence in the result, ten repeat runs were carried out. Detailed results, defining the resulting pulses are given in Appendix 1. From the result in Figure 11, it is noted that the $n=2$ case of the n -step series runs is above the optimal two-step result. In theory this should be the case since the $n=2$ case has less flexibility with its two segments required to be equal.

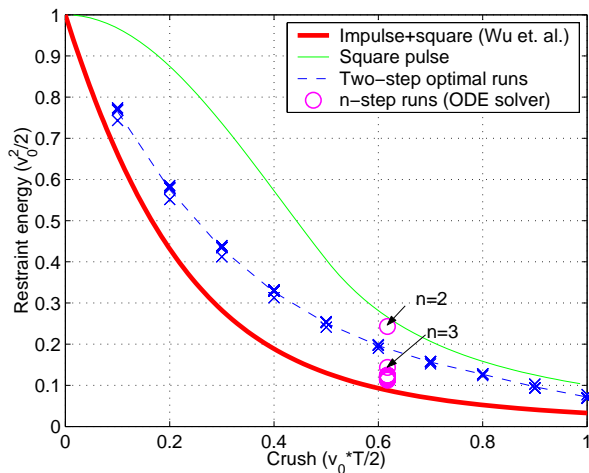


Figure 11. Occupant restraint energy and crush pulse relationship for theoretical and numerical examples (The dash line connects the average of results of ten repeat runs (each represented by an 'x') at each normalized crush for the two-step optimization. Also see Figure 1 for notes on definition of variables).

Convergence to Local Minima

The lack of global convergence as shown in the numerical examples warrants a discussion. Convergence to local minima is an unpleasant reality with many complex nonlinear optimization problems. For each particular problem, its significance should be assessed in light of the overall objective. For example, in the case of the n -step example problem here, if the objective is a theoretical study of the functional optimization problem, the local convergence is a severe obstacle, since one would want to be able to find the solution as n increases to infinity. On the other hand, if the objective is to achieve simply an improvement, the SQP/GA algorithm apparently is still of value.

Quantitatively, from Figures 4, 8a, and 9a, it appears reasonable to assume high confidence in the quality of result from a single optimization run, if the number of segments does not exceed 4 or 5. This may appear to be rather restrictive; however, from a practical point of view, this condition is of limited significance for the following reasons. First, an analysis based on such SDOF spring-mass models is for guidance in general, and rigorous convergence requirement is not meaningful. Second, limiting the number of segments is sensible, because an optimal pulse target will invariably be only approximately realized in practice, because of the complexity in both the vehicle structure and crush dynamics. Therefore, the numerical optimization method can be applied to practical design process, with a numerical effectiveness consistent with the efficacy of the simple vehicle-occupant model.

SUMMARY AND CONCLUSIONS

The notion of an optimal pulse is only meaningful when the constraint conditions are specified clearly. The pulse identified by Wu et al. [1] represents a theoretical optimum under non-negative pulse constraint. The optimal pulse problem may be solved numerically with a formal optimization approach, when complex constraints are present. The current work provides one solution scheme.

The vehicle pulse is discretized in the vehicle crush domain, and the optimal acceleration levels are determined through a numerical search scheme. The search scheme is a hybrid of the SQP and GA search methods. The SQP search, although more efficient, needs assistance from the GA search to alleviate the local convergence problem. The hybrid SQP/GA scheme still does not guarantee global convergence. However, when the number of pulse discretization segments is less than five, the method is effective in providing pulse improvements for practical problems.

ACKNOWLEDGEMENT

The authors wish to thank Dr. Guglielmo Rabbio of DaimlerChrysler for his suggestion for using the scaling scheme to impose the constraint in the GA algorithm.

REFERENCES

- [1] Wu, J., G. S. Nusholtz, and S. Bilkhu. 2002. "Optimization of Vehicle Crash Pulses in Relative Displacement Domain". Int. Journal of Crashworthiness, pp. 397-413, Vol. 7, No. 4.
- [2] Egli, A. 1968. "Stopping the Occupant of a Crashing Vehicle - A Fundamental Study". SAE Transactions, Vol. 76.
- [3] Searle, J. 1970. "Optimum Occupant Restraint". SAE 700422.
- [4] Lundell, B. 1984. "Dynamic Response of a Belted Dummy - A Computer Analysis of Crash Pulse Variation". SAE 840401.
- [5] Ishii, K. and I. Yamanaka. 1988. "Influence of Vehicle Deceleration Curve on Dummy Injury Criteria". SAE 880612.
- [6] Brantman, R. 1991. "Achievable Optimum Crash Pulses for Compartment Sensing and Airbag Performance". SAE 916148, 13th International Technical Conference on Experimental Safety Vehicles, S9-O-22.
- [7] Matsumoto, H, et al. 2000. "A parametric Evaluation of Vehicle Crash Performance". SAE 900465.
- [8] Grims, W. and F. D. Lee. 2000. "The Effect of Crash Pulse Shape on Occupant Simulation". SAE 2000-01-0460.
- [9] Whittman, W. J. and R. F. C. Kriens. 1999. "Numerical Optimization of Crash Pulses". EUROPAM 99 -- 9th User Conference.
- [10] Takahashi, K. et al. 1993. "Optimization of Vehicle Deceleration Curves for Occupant Injury". SAE 9307515.
- [11] Motozawa, Y. and T. Kamei. 2000. "A New Concept for Occupant Deceleration Control in a Crash". SAE 2000-01-0881.
- [12] Papalambros, P. Y., and D. J. Wilde. 1988. "Principles of Optimal Design: Modeling and Computation". Cambridge University Press.
- [13] MathWorks. 1996. "Matlab Optimization Toolbox, Version 1.5".

- [14] Goldberg, D. E. 1989. "Genetic Algorithms in Search, Optimization, and Machine Learning". Addison-Wesley.

APPENDIX 1. RESTRAINT ENERGY V.S. VEHICLE CRUSH OF EXAMPLE PULSES WITH LINEAR RESTRAINT

Equations for the restraint energy v.s. vehicle crush relationships plotted in Figures 1 and 11 for the example pulses are given here. The equations are derived using either direct solution of equation of motion, or the energy relationship in [1]. In this appendix, c denotes the vehicle crush normalized by $v_0 T/2$ (the vehicle crush for a square-pulse with the natural period T of the restraint system as the duration), and e denotes the occupant restraint energy normalized by $v_0^2/2$ (the restraint energy resulted from an impulse pulse with v_0 velocity change).

Impulse+Square pulse by Wu et al. [1]

$$c = \frac{\beta}{2} \left(1 + \frac{\beta}{\pi(1-\beta)} \right), \quad e = (1-\beta)^2 \quad (\text{A1.1})$$

where β is a parameter (the ratio of the velocity changes in the square part of the pulse to the crash velocity).

Two-impulse pulse

When the second impulse occurs at time $t_e = T/4$ (T is the period of the linear restraint system):

$$c = \frac{1}{2} \beta, \quad e = \beta^2 + (1-\beta)^2 \quad (\text{A1.2}),$$

where β is a parameter (the ratio of the velocity changes of the second impulse to the total velocity change).

When the second impulse is allowed to occur at a time $t_e > T/4$,

$$c = \frac{\omega t_e}{\pi} \beta, \quad e = (1-\beta)^2 \quad (\text{A1.3}),$$

where $\beta \leq 2/3$ is defined the same as in the first case, and ω is the radian frequency of the linear restraint system. The time at which the second impulse should be applied to achieve the best among the two-impulse cases is determined by:

$$\cos(\omega t_e) = -\frac{\beta}{2(1-\beta)} \quad (\text{A1.4}).$$

Note that in this case, unloading-reloading of the restraint occurs before the second impulse.

"Cosine type" pulse by Motozawa et al. [11]

$$c = \frac{2 - \beta^2}{4(1 - \beta)} \alpha - \frac{2(1 - \beta)}{\pi^2} \left(\frac{1}{\alpha^2} - 1 \right) \alpha, \quad e = 4 \left(\frac{1 - \beta}{\alpha \pi} \right)^2 \quad (A1.5),$$

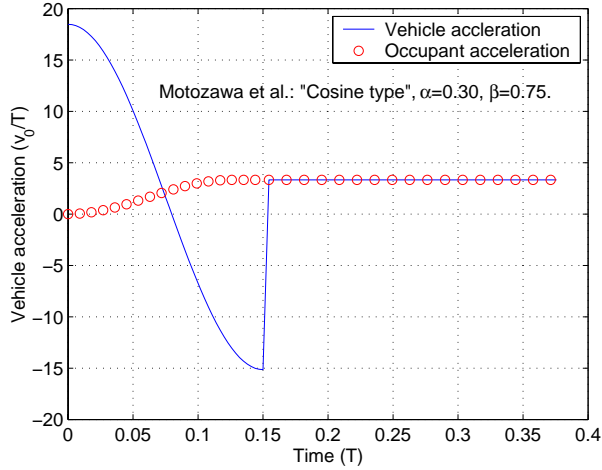


Figure A.1. Example of "Cosine type" occupant acceleration and corresponding vehicle pulse by Motozawa and Kamei [11]. (This example enters the curve in Figure 1 with normalized restraint energy at 0.28. The vehicle acceleration is required to have a period of significant negative acceleration.)

where β is a parameter (the ratio of the velocity change of the square part of the pulse to the total velocity change). α is another free parameter. The time for the start of the square part of the pulse, t_c , is determined by $\alpha = \omega t_c / \pi$, where ω is the radian frequency of the linear restraint system. In the example plotted in Figure 1, $\alpha=0.30$. Its time histories for the vehicle and occupant accelerations are shown in Figure A1.

Square pulse

When the duration of the square pulse is less or equal to half of the natural period of the linear restraint system, the solution is:

$$c = \frac{\beta}{2\pi}, \quad e = \left(\frac{2}{\beta} \sin \frac{\beta}{2} \right)^2 \quad (A1.6),$$

where β is a parameter. The ending time of the pulse, t_e , is determined by $\beta = \omega t_e$, where ω is the radian frequency of the linear restraint system.

Two-step pulse

The optimal two-step pulse solution was obtained using the numerical optimization method in this study. The optimal occupant response is shown in Figure 11. More computation details are given in Tables A.1a and A.1b, which define the actual pulse for each of the runs performed.

Table A.1a Ratio of second to first crush segments

Normalized crush	0.1	0.2	0.3	0.4	0.5	0.6	0.7	0.8	0.9	1.0
Run 1	0.80	0.83	0.86	0.88	0.91	0.92	0.94	0.95	0.16	0.16
2	0.80	0.83	0.86	0.88	0.91	0.92	0.94	0.95	0.16	0.16
3	0.80	0.83	0.86	0.88	0.91	0.92	0.94	0.95	0.16	0.16
4	0.80	0.83	0.86	0.88	0.91	0.92	0.94	0.95	0.16	0.16
5	0.77	0.80	0.84	0.87	0.89	0.91	0.93	0.08	0.14	0.18
6	0.77	0.80	0.84	0.87	0.89	0.91	0.93	0.08	0.14	0.21
7	0.79	0.81	0.85	0.88	0.90	0.92	0.93	0.95	0.16	0.18
8	0.80	0.82	0.85	0.88	0.90	0.92	0.94	0.95	0.20	0.25
9	0.93	0.94	0.95	0.96	0.97	0.98	0.98	0.98	0.99	0.24
10	0.93	0.94	0.95	0.96	0.97	0.98	0.98	0.98	0.99	0.24

Table A.1b Ratio of second and first step of acceleration

Normalized crush	0.1	0.2	0.3	0.4	0.5	0.6	0.7	0.8	0.9	1.0
Run 1	0.801	0.827	0.856	0.885	0.907	0.924	0.939	0.950	0.157	0.164
2	0.801	0.827	0.856	0.885	0.907	0.924	0.939	0.950	0.157	0.164
3	0.801	0.827	0.856	0.885	0.907	0.924	0.939	0.950	0.157	0.164
4	0.801	0.827	0.856	0.885	0.907	0.924	0.939	0.950	0.157	0.164
5	0.772	0.800	0.835	0.866	0.893	0.913	0.930	0.081	0.140	0.183
6	0.772	0.800	0.835	0.866	0.893	0.913	0.930	0.081	0.140	0.207
7	0.787	0.814	0.846	0.875	0.899	0.920	0.934	0.945	0.156	0.180
8	0.796	0.823	0.853	0.882	0.904	0.923	0.937	0.949	0.200	0.248
9	0.935	0.944	0.954	0.963	0.970	0.976	0.980	0.984	0.986	0.242
10	0.935	0.944	0.954	0.963	0.970	0.976	0.980	0.984	0.986	0.242

APPENDIX 2. ANALYTICAL SOLUTION OF VEHICLE AND OCCUPANT ACCELERATION TIME HISTORIES WITH N-STEP-PULSE AND LINEAR ELASTIC RESTRAINT

Refer to Figure 3, the vehicle velocity at the end of the i -th step can be calculated through:

$$v_i^2 = v_{i-1}^2 - 2a_i \Delta x_i \quad (i=1 \dots n) \quad (\text{A2.1}),$$

where a_i and Δx_i are the acceleration level and the crush of the i -th segment, and v_0 is the vehicle initial velocity. The time duration for the segment is:

$$\Delta t_i = \frac{2\Delta x_i}{v_{i-1} + v_i} \quad (i=1 \dots n) \quad (\text{A2.2}).$$

With Δt_i and a_i , the vehicle acceleration time history is known.

In each of the segment, the occupant response is that of a forced linear system described by:

$$\ddot{y}(t) + \omega^2 y(t) = a_i \quad (t_{i-1} \leq t \leq t_i) \quad (\text{A2.3}),$$

where y is the relative displacement between the occupant and the vehicle at a given time t that falls between the beginning of the i -th segment (t_{i-1}), and its end (t_i). These times are already available from Equation A2.2. ω in Equation A2.3 is the radian frequency of the system consisting of the occupant and the linear elastic restraint.

The solution for A2.3 is:

$$y(\bar{t}_i) = c_{1i} \sin(\omega \bar{t}_i) + c_{2i} \cos(\omega \bar{t}_i) + a_i / \omega^2 \quad (\text{A2.4a}),$$

$$(0 \leq \bar{t} \leq \Delta t_i, i = 1 \dots n)$$

where $\bar{t}_i = t - t_{i-1}$ is a shifted time for convenience.

The relative velocity and acceleration are accordingly:

$$\dot{y}(\bar{t}_i) = c_{1i} \omega \cos(\omega \bar{t}_i) - c_{2i} \omega \sin(\omega \bar{t}_i), \quad (\text{A2.4b}),$$

$$(0 \leq \bar{t} \leq \Delta t_i)$$

and,

$$\ddot{y}(\bar{t}_i) = -c_{1i} \omega^2 \sin(\omega \bar{t}_i) - c_{2i} \omega^2 \cos(\omega \bar{t}_i) \quad (\text{A2.4c}).$$

$$(0 \leq \bar{t} \leq \Delta t_i)$$

The initial conditions are:

$$y(\bar{t} = 0) = y_{i-1}, \quad \dot{y}(\bar{t} = 0) = \dot{y}_{i-1} \quad (\text{A2.5}),$$

where y_{i-1} and \dot{y}_{i-1} are the displacement and velocity at the beginning of the i -th segment. Since the occupant and the vehicle are moving together at the incipience of the crash, we have:

$$y_0(0) = 0, \quad \dot{y}_0(0) = 0 \quad (\text{A2.6})$$

Using the above initial conditions, for each segment, the constants in A2.4 can be computed:

$$c_{1i} = \dot{y}_{i-1} / \omega, \quad c_{2i} = y_{i-1} - a_i / \omega^2. \quad (\text{A2.7})$$

Therefore, stepping through from $i=1$ to n , Equations A2.7 and A2.4 can be used to progressively solve for the complete time history of the occupant. When needed, the absolute acceleration of the occupant is found by:

$$\ddot{z}(t) = -\ddot{y}(t) + a_i \quad (t_{i-1} \leq t \leq t_i) \quad (\text{A2.8})$$